EUROPEAN FUSION DEVELOPMENT AGREEMENT

EFDA–JET–PR(03)40

D.C. McDonald, J.G. Cordey, E. Righi, F. Ryter, G. Saibene, R. Sartori, B. Alper, M. Becoulet, J. Brzozowski, I. Coffey, M.de Baar, P.de Vries, K. Erents, W. Fundamenski, C. Giroud, I. Jenkins, A. Loarte, P. J. Lomas, G.P. Maddison, J. Mailloux, A. Murari, J. Ongena, J. Rapp, R.A. Pitts, M. Stamp, J. Strachan, W. Suttrop and JET EFDA contributors

ELMy H-modes in JET Helium-4 Plasmas

ELMy H-modes in JET Helium-4 Plasmas

D.C. McDonald[1], J.G. Cordey[1], E. Righi[2a], F. Ryter[3], G. Saibene[2], R. Sartori[2], B. Alper[1], M. Becoulet[4], J. Brzozowski[5], I. Coffey[6], M.de Baar[7], P.de Vries[1, 7], K. Erents[1], W. Fundamenski[1], C. Giroud[7], I. Jenkins[1], A. Loarte[2], P. J. Lomas[1], G. P. Maddison[1], J. Mailloux[1], A. Murari[8], J. Ongena[9], J. Rapp[8], R. A. Pitts[10], M. Stamp[1], J. Strachan[11], W. Suttrop[3] and JET EFDA contributors*

[1]EURATOM/UKAEA fusion association, Culham Science Centre, Abingdon, Oxon, OX14 3DB, UK
[2]EFDA Close Support Unit, D-85740 Garching, Germany
[3]Max Planck Institut für Plasmaphysik EURATOM Association, D-85740 Garching, Germany
[4]Association EURATOM-CEA, CEA Cadarache, F-13108, St Paul lez Durance, France
[5]Association EURATOM-VR, KTH Royal Institute of Technology, Se-100 44 Stockholm, Sweden
[6]Department of Physics, Queen's University, Belfast, UK
[7]FOM-Instituut voor Plasmafysica 'Rijnhuizen', Associatie Euratom-FOM, Trilateral Euregio Cluster, P.O. Box 1207, 3430 BE Nieuwegein, the Netherlands
[8]EFDA-JET CSU, Culham Science Centre, Abingdon, Oxon, OX14 3EA, UK
[9]LPP-ERM/KMS Association Euratom-Belgian State, Brussels, Belgium
[10]CRPP Association EURATOM-Confédération Suisse, École Polytechnique Fédérale de Lausanne, CH-1015 Lausanne, Switzerland
[11]PPPL, Princeton University, Princeton NJ, 08543, USA
[a]Current address: European Comission, Brussels
** See annex of J. Pamela et al, "Overview of Recent JET Results and Future Perspectives", Fusion Energy 2000 (Proc. 18th Int. Conf. Sorrento, 2000), IAEA, Vienna (2001).*

Preprint of Paper to be submitted for publication in
Plasma Physics and Controlled Fusion

ABSTRACT

ELMy H-modes in helium-4 plasmas provide valuable information on ELMy H-mode physics as well as a possible early low activation operational phase for next-step tokamaks, such as ITER. With this in mind a series of helium-4 H-mode experiments were performed on JET with pure helium-4 NBI auxiliary heating (up to 12MW). A set of ELMy H-mode plasmas were produced, in both the Type I ELM regime and a second regime, which showed similar characteristics to the deuterium Type III regime, but with the reverse ELM frequency dependence on power. Sawteeth were also observed, and had similar behaviour to those seen in deuterium. Compared with deuterium plasmas, Type I ELMy H-mode confinement is seen to be 28±6% poorer in helium-4 plasmas and the L-H power threshold 42±10% larger. This is the opposite of the behaviour predicted by experimental isotope mass scalings from hydrogenic plasmas. Comparison with a wider hydrogenic database, enables the effects of isotopic charge and mass to be studied independently.

1. INTRODUCTION

The study of H-modes in helium-4 plasmas offers valuable information for the understanding of edge and divertor physics, core confinement, pedestal physics, the L-H threshold, ELMs and sawteeth. Operation in helium-4 also provides a possible early low activation operational phase for next-step tokamaks, such as ITER. However, with the exception of a short campaign on the DIII-D facility [1], which used deuterium Neutral Beam Injection (NBI), few helium H-mode experiments have been carried out in large, diverted tokamaks. With this in mind, helium-4 experiments (with helium-4 plasmas up to 95% pure) were carried out on JET, with the Mark IIGB divertor. This paper presents results on the study of the L-H mode threshold, ELM and sawtooth behaviour, and energy confinement in helium-4 plasmas. They represent the first systematic study of the L-H threshold and ELMy H-modes in helium-4 plasmas in a large, diverted tokamak, and provide the first measures of the isotope charge dependence of the L-H threshold, ELMy H-mode confinement, ELM Type, and sawtooth period in ELMy H-mode regimes. Results concerning the edge and divertor physics are reported elsewhere [2, 3].

This paper is structured as follows: Section 2 outlines some relevant details of operating JET in helium-4 plasmas. Section 3 concerns the impact of helium plasmas upon the conditions for L-H transitions. The behaviour of ELM's and sawteeth in helium-4 plasmas is discussed in section 4. The confinement properties of both Type I and Type III ELMy H-mode plasmas are studied in section 5. Finally, the results are summarised and discussed in section 6. For the majority of the analyses, the behaviour of helium plasmas is compared with that of deuterium plasmas, which are used for the bulk of operation in modern tokamaks.

2. OPERATION IN HELIUM

Operation in helium presented many technical difficulties, most notably for Neutral Beam Injection (NBI) heating and divertor operation. For auxiliary heating, the NBI sources were converted to

helium-4, and successfully coupled up to 12 MW of power to the plasmas. However, the increased L-H threshold in helium-4 (see section 3), limited the toroidal field and plasma current for which H-modes could be achieved. Argon frosting of the Mark II GB divertor enabled the pumping of helium but did reduce the number of discharges that could be run in a day. A small (<2MW) additional amount of minority hydrogen ICRH heating [4] was also used in some of the discharges studied in this paper.

Despite argon frosting, the rate at which the divertor pumped helium-4 for the helium-4 discharges remained lower than the rate it pumped deuterium in the reference discharges [2]. This resulted in a steady increase in the divertor neutral density, except for plasmas with the lowest current and power. Although most of the deuterium in the near surface wall reservoir was removed by helium-4 bombardment during the first helium-4 discharge, significant amounts of deuterium remained more deeply embedded [5]. As a result, deuterium continued to be desorbed from the walls during high power Type I ELM phases, which is believed to be due to the large heat loads during ELM crashes at the strike points and main chamber wall surfaces. This resulted in a lower helium-4 ion purity in Type I ELMy H-modes (65%-86%), compared with that of the Type III ELMy H-modes (87%-95%). The lack of helium chemistry, resulting in the absence of deuterium chemical sputtering on the carbon surfaces of the first wall, meant that, in general, the helium plasmas had lower levels of carbon impurities [2,6] than would be the case in hydrogenic plasmas.

Helium-4 concentrations were calculated from the He-I and Dα spectroscopic lines, with a constant concentration profile assumed. Photon efficiencies were also assumed constant. The low values of neutron emission in the helium-4 discharges (less than 1.1×10^{11} $m^{-3}s^{-1}$ in all cases) were consistent with the helium-4 concentration estimates from visible spectroscopy being within 20% of the true value. Neutral beam power absorption, calculated by the PENCIL [7] code, has a reduced confidence due to the higher uncertainty in helium-4 cross-section measurements relative to hydrogenic ones [8]. Global thermal energy measurements, made by subtracting the fast particle energy calculated by PENCIL from the stored energy measured by magnetic coils, were similarly affected. These were found to be consistent with those calculated from density and temperature measurements. Further analysis of plasma diagnosis from JET operation in helium-4 is reported elsewhere [9, 10].

3. L-H THRESHOLD

The L-H threshold experiments were performed in JET, operating with the Mark IIGB divertor, in single null configurations with the ion-gradB drift towards the X-point. Configuration, magnetic field, current and q-profiles were varied between discharges. The configurations were low shape (κ=1.58-1.68, δ=0.18-0.25), with the X-point typically 7-10cm above the septum, but varying from 5cm below to 13cm above the septum for the dedicated X-point scans (section 3.3). Magnetic fields varied from 1.0-3.45T, plasma currents from 1.0-3.2T, and q_{95} (the safety factor of the surface containing 95% of the poloidal flux of the last closed flux surface) from 2.9-3.8. Line averaged

electron densities varied from 1.5-3.9×10^{19} m^{-3}. The L-H power threshold was measured using a NBI only linear power ramp [11], with a ramp rate slow enough ($dP_{NBI}/dt < 1.5\,MWs^{-1}$ in all experiments, where P_{NBI} is the coupled NBI power) to ensure that, prior to the L-H transition, the key plasma parameters were varying on a slow time scale compared with the plasma energy confinement time ($dW_{th}/dt\tau_E < 0.2W_{th}$ and $d\bar{n}_e/dt\tau_E < 0.3\bar{n}_e$ and in all cases, where W_{th} is the plasma thermal energy, $\bar{n}_e$ is the line averaged electron density, and τ_E is the energy confinement time). The relatively low divertor power loads of L-mode plasmas, together with the shortness of the auxiliary heating duration before the L-H transition (typically <2s), meant that deuterium concentrations were lower for the L-H threshold experiments than for the Type I ELMy H-mode confinement experiments (see section 5). For all the discharges, helium-4 concentrations were in the range 84-94%.

3.1 DENSITY AND POWER

For the same q_{95} (≈3.3) and configuration, helium-4 and deuterium reference discharges were performed at a range of toroidal magnetic fields (1-3.2 T). During the power ramps for these shots, no gas was injected into the plasmas, but shots taken with and without argon frosting on the divertor tiles and the NBI cryopanels gave a natural variation in density. The small variations in plasma geometry in the experiments (a = 0.96, R_0 = 2.83-2.90; where a is the plasma minor radius in m and R_0 is the plasma major radius in m) mean that the dependence of the L-H threshold on major and minor radius cannot be studied. For deuterium plasmas, It has been shown [12] that the observed L-H power thresholds, derived from a multi-machine H-mode power threshold database [13], are consistent with the expression

$$P_{L\text{-}H}^{D,scal} = 0.87\,\bar{n}_e^{0.77}\,B_0^{0.92} \qquad (1)$$

where, $P_{L\text{-}H}$ is the loss power, P_{loss}, at the L-H transition in MW, $\overline{n_e}$ is the line averaged electron density in 10^{19} m^{-3}, B_0 is the vacuum magnetic field at the plasma centre in T, $P_{loss} = P_{IN} - \dot{W}_{th}$ is the loss power across the separatrix, P_{IN} is the total ohmic and auxiliary power coupled to the plasma, and the mean values of minor and major radius for the L-H threshold experiments at JET (a=0.96, R_0=2.87) have been applied. Figure 1 shows the observed power thresholds plotted against equation 1. The deuterium reference discharges fit the scaling with a RMSE of 15.2%. A direct fit of the helium-4 power threshold data to line averaged density and magnetic field gives

$$P_{L\text{-}H}^{He\text{-}4} = (1.23\pm0.13)\,\bar{n}_e^{0.77\pm0.17}\,B_0^{0.92\pm0.12} \qquad (2)$$

Comparison with (1) shows that the power law scalings for density and field in helium-4 plasmas are identical with those of the scaling law for deuterium to two decimal places. With this fit, the helium-4 data (9 discharges) has a RMSE of 11.6%. Given the uncertainties in these measurements, the high degree of agreement in the exponents is clearly coincidental, but it is apparent that the

power law scalings for density and field in helium-4 plasmas are consistent with those for deuterium plasmas within the error bars. However, the coefficient in (2) corresponds to a higher L-H power threshold for a helium discharge compared to that predicted for a deuterium discharge by (1). We note that other, more recent, multi-machine scalings for the L-H threshold power of deuterium H-modes [14, 15] also fit the helium-4 and deuterium reference data of this paper, within error bars, but with a higher RMSE.

The increase of L-H power threshold below a critical density, seen in earlier deuterium experiments on JET and several other tokamaks [16, 17, 18, 19, 20, 21], was not observed in helium-4 plasmas. This indicates that, if such a critical density exists for helium-4 discharges at JET, it lies below the densities studied ($\bar{n}_e > 1.5\times10^{19}$ for all helium-4 L-H transitions). In deuterium JET plasmas, the critical density was found to be $\bar{n}_e = 1-1.4\times10^{19}$ [22, 21].

3.2 ISOTOPE EFFECT

As, when compared with hydrogenic plasmas, there is no evidence for the L-H power threshold in helium-4 plasmas having a separate density and magnetic field scaling, the L-H power threshold of the helium-4 plasmas studied may be taken to be of the form of Equation 1. If this is the case, the L-H power threshold of helium-4 plasmas relative to deuterium plasmas may be written as

$$P_{L\text{-}H}^{He\text{-}4} = (1.42\pm0.10)\, P_{L\text{-}H}^{D} \tag{3}$$

The L-H threshold is seen to be around 42% higher than that of deuterium. A log-linear fit with atomic charge and mass, including the earlier hydrogen, deuterium, deuterium-tritium and tritium data [23, 24], results in

$$P_{L\text{-}H} = M^{-1.1} Z^{1.6} P_{L\text{-}H}^{D,scal} \tag{4}$$

Where, M and Z are the mean isotope mass and charge, scaled to that of a proton. Thus, the power threshold for a helium-4 plasma would be significantly (52%) below that of its hydrogen equivalent. Thus, for the low activation phase of a next step machine, the experiments suggest that the H-mode would be easier to access in helium-4 plasmas than in hydrogen ones.

Kiviniemi et al [25] have shown theoretically that this isotope dependence may be explained by a neoclassically driven edge electric field stabilising edge turbulence through E×B shear. Hidalgo et al [26] have shown that the isotope dependence to be consistent with a model based on turbulent transport which is self-regulated by fluctuations.

3.3 PLASMA CONFIGURATION

Following JET Mark IIGB deuterium plasma experiments [27, 28], where the height of the X-point above the septum was shown to alter the L-H power threshold by a factor of 2, a similar scan was repeated in helium-4. Figure 2 shows the range of configurations studied, with X-point heights varying between 5cm below and 13cm above the septum. The trend seen in deuterium was reproduced in

helium-4 plasmas, Figure 3, with the L-H power threshold with the X-point on the septum being close to half that of L-H transitions with the X-point 6cm above the septum. P_{L-H} (0cm)/P_{L-H}(6cm) = 0.54 in helium-4, and P_{L-H} (0cm)/P_{L-H}(6cm) = 0.61 in the deuterium references for the dedicated discharges. X-points more than 6cm above the septum, the dependency disappears. This behaviour is not understood but, as earlier JET results in deuterium [27] showed an associated fall in the edge electron temperature immediately prior to the L-H transition for the same edge density and field, it is inconsistent with transition models based solely on fully ionised plasma physics. As such, the results would appear to support models involving neutral penetration, although such models must explain why helium-4 and deuterium plasmas show similar trends in threshold dependence when they possess different ionisation properties. Plasma edge measurements for the helium-4 L-mode plasmas [2] indicated that the electron density and temperature profiles in the scrape of layer were similar to their deuterium references.

4 ELM AND SAWTOOTH BEHAVIOUR

4.1 TYPE I ELMS

Type I ELMs were obtained in a range of configurations and currents ($1.0 \leq I_p \leq 2.0$; where I_p is the plasma current in MA). The ELM frequencies were relatively low (15Hz-45Hz). In all cases the ELM crashes were clearly defined peaks with strong correlation between the inner and outer divertor He-I line emission. Figure 4 shows the results of a NBI only power scan for a 1MA/1T helium-4 plasma in a low triangularity ($\delta \approx 0.25$), standard septum clearance (X-point 7cm above the septum) configuration. As the injected NBI power increases across the scan from 6.3MW to 10.1MW, the ELM frequency increases monotonically from 17Hz to 50Hz. Thus, the ELM behaviour is in accordance with that shown in Type I ELMs in hydrogenic gases [29, 30]. During these Type I ELM crashes in helium-4, the energy loss per ELM, ΔW_{ELM}, lay in the range $\Delta W_{ELM}/W_{th}$=5-9%, and the time averaged power loss per ELM, P_{ELM}, in the range P_{ELM}/P_{loss}=16-25%. For the deuterium reference Type I ELMy H-modes, the energy loss per ELM lay in the range $\Delta W_{ELM}/W_{th}$=4-9%, and the time averaged power loss per ELM in the range P_{ELM}/P_{loss}=20-33%.

4.2 TYPE III ELMS

At lower powers and/or lower densities, a second ELM regime was observed. The observed ELM frequencies (30 Hz – 170 Hz) were higher than for the Type I ELM's, but the He-I amplitudes at the crashes were smaller and showed less clearly defined peaks. The energy confinement of the plasmas in these regimes was also lower than that for Type I ELM's (see section 5). In several helium-4 discharges, with decreasing power or increasing density, a direct transition from the Type I to the second regime was observed, with an abrupt change in ELM frequency and amplitude. As all of these features are common to Type III ELM's observed in hydrogenic JET plasmas [29, 30], they shall be identified here as Type III ELM's in helium-4.

However, the response of the frequency of Type III ELM's in helium-4 to power, often taken as the signature of Type III ELM's in hydrogenic plasmas, is different. Figure 5 shows the results of a NBI only power scan experiment for a 1.5MA/1.5T helium-4 plasma in a low triangularity ($\delta \approx 0.2$), high septum clearance (X-point 20cm above the septum) configuration. Once again, as the NBI power is raised (from 6.0 MW to 9.7 MW), the ELM frequency rises monotonically (from 80 Hz - 160 Hz). This is the reverse of the trend observed in Type III ELM's in hydrogenic plasmas [29, 30] and was observed in all helium-4 Type III ELMy H-mode discharges where power was varied (6 discharges). Although, no specific experiment to study the Type III-ELM free transition was performed, two discharges did show this transition. Although, in both cases injected power was switched on directly, without a ramp, it is reasonable to assume that the power through the separatrix increased on the time scale of the beam slowing down time and the energy confinement time. In both discharges then, ELM frequency (in the range 1-2 kHz) increased with input power, consistent with the above trend for Type III ELM's in helium-4, and then fell discontinuously before the ELM free period.

Figure 6 shows the relation between the ELM frequency and the loss power relative to the predicted loss power for the L-H transition in helium-4 (Equation 3), for a database of helium-4 Type I, Type III and Type I-III discharges. As for JET deuterium plasmas [31], all the Type III ELMy H-mode discharges have loss powers below twice that of the L-H threshold. Similarly, Type I ELMy H-modes are seen at higher powers ($P_{loss} > 1.6 P_{L-H}$ in all cases). The wide scatter in ELM frequency for the Type III ELMy H-modes implies that parameters other than power, such as plasma current, field, density and configuration, affect the ELM frequency. For the high triangularity ($\delta = 0.4$) plasmas, Type III ELMs were seen at generally lower powers ($P_{loss}/P_{L-H} = 0.7\text{-}1.2$), and a set of compound Type I-III ELMy H-mode plasmas were observed at loss power levels between 10% and 30% above the L-H threshold, suggesting a somewhat lower Type I-III transition threshold. This is consistent with the effect of triangularity observed in JET deuterium discharges [32, 31].

4.3 SAWTEETH

Although there is no generally accepted formula or empirical scaling for the sawtooth period of a plasma, de Vries et al [33] found the following fit to the sawtooth period in ms, $\tau_{sawtooth}^{Scal,D}$, for a range of JET Mark IIGB deuterium plasmas with NBI only auxiliary heating,

$$\tau_{sawtooth}^{Scal,D} = 20 n_{e0}^{0.23} T_{e0}^{1.69} \qquad (5)$$

Where n_{e0}, the core electron density in $10^{19} m^{-3}$, and T_{e0}, the core electron temperature in keV, are taken immediately before the sawtooth crash. Both the Type I helium-4 ELMy H-modes and their deuterium references give a reasonable fit to this scaling (Figure 7) with very little sign of an isotope dependence in the absolute value. A direct fit of the data to (5) gives,

$$\frac{\tau_{sawteeth}^{He\text{-}4}}{\tau_{sawteeth}^{He\text{-}4}} = (0.98 \pm 0.11) \frac{\tau_{sawteeth}^{D}}{\tau_{sawteeth}^{Scal,\,D}} . \qquad (6)$$

It has also been found that large, ICRH driven, fast energy helium-4 populations can stabilise sawteeth [34], in the same manner as in deuterium. Neoclassical Tearing Modes, which can be triggered by sawteeth on JET, were not seen in any of the confinement or threshold discharges analysed in this paper.

5. ENERGY CONFINEMENT

The energy confinement of the Type I ELMy H-mode and Type III ELMy H-mode in helium-4 discharges of section 4 has been studied. As discussed in section 2, the relative inefficiency of the Mark IIGB divertor at pumping helium-4, when compared to deuterium, led to a continual rise in deuterium concentration throughout the discharges. Figure 8 shows a typical helium-4 Type I ELMy H-mode confinement discharge, with the divertor neutral density increasing throughout the auxiliary heating phase, as seen by the rise in the edge divertor light. This is associated with a rise in line averaged density and a fall in the ELM frequency. A "steadiness" criterion of $\tau_{divlight} < 5\tau_E$, where $\tau_{divlight}$ is the time taken for the He-I divertor light signal to double in magnitude, was introduced to ensure the pulses used were steady over several confinement times. Z, the mean ion charge was used to describe the relative concentrations of helium-4 and deuterium in the plasmas.

5.1 TYPE I ELMS

Four steady, Type I ELMy H-modes were produced, all at $q_{95} \approx 3.3$, with plasma currents of 1MA and 2MA, and densities in the range 55-75% of the Greenwald density limit [35] (The H-mode density limit in helium-4 ELMy H-modes being close to that seen in deuterium [36]). Helium-4 NBI heating (6-11MW) was used with some additional 2nd harmonic hydrogen minority ICRH (2MW) in one discharge. The relatively low number of discharges meant that the dependence of helium-4 energy confinement on current, density and power could not be obtained. However, as a set of reference deuterium plasmas were produced, it is possible to study the isotope dependence.

Figure 8 shows the time evolution of one of the helium-4, 1MA/1T, Type I ELMy H-modes compared with that of its deuterium reference. It can be seen that the higher H-mode threshold in helium-4, discussed in section 3, means that a higher input power was required to achieve Type I ELMs for the helium-4 discharge. The resulting plasmas were, however, well matched for electron density and ELM frequency. The energy confinement, for a wide range of hydrogenic plasmas, has been shown to be consistent with the IPB98(y,2) scaling [12],

$$\tau_{IPB98(y,2)} = 5.62\times10^{-2}\, P_{loss}^{-0.69}\, B_0^{0.15}\, I_P^{0.93}\, \kappa^{0.78}\, \bar{n}_e^{0.41}\, a^{0.58}\, R^{1.39}\, M^{0.19} \qquad (7)$$

where $\tau_{IPB98(y,2)}$ is the energy confinement time in seconds. The mass dependence means that the scaling predicts that energy confinement in helium-4 plasmas would be 14% higher than in deuterium. It can be seen from figure 8, however, that this was not the case, with the stored energy for the helium-4 plasma lying below that of its deuterium reference, despite the 70% higher injected power.

Figure 9 shows the energy confinement time, scaled to IPB98(y,2), for the full set of helium-4 Type I ELMy H-modes and their deuterium references. All discharges are in a low triangularity ($\delta \approx 0.2$), standard septum clearance (X-point 8cm above the septum) configuration with q_{95}=3.3, and I_p= 1-2.6MA. The deuterium references themselves contain small concentrations of helium-4 (9%-21%). The helium-4 discharges can clearly be seen to have lower energy confinement with a mean scaled energy confinement time ($H_{IPB98(y,2)} = \tau_E/\tau_{IPB98(y,2)}$) of 0.77±0.04 compared with 1.07±0.04 for the deuterium discharges. This can be represented by introducing a mean ion charge dependency of the form,

$$\tau_E = Z^{-0.75\pm0.08}\,\tau_{IPB98(y,2)}, \tag{8}$$

where it should be remembered that the IPB98(y,2) scaling has a mass dependence of $M^{0.19\pm0.05}$. The energy confinement time of a pure helium-4 plasma relative to a pure deuterium plasma with all other engineering plasmas, including electron density, constant is thus estimated as $\tau_E^{He\text{-}4}/\tau_E^{D}$= 0.68±0.08. Figure 10 shows the confinement time for a set of discharges that include hydrogen and tritium plasmas [37]. The energy confinement time has been normalised to the IPB98(y,2) scaling, with the isotope mass dependency removed to enable the absolute plasma performance of each isotope species to be compared. Once again, all discharges are in a low triangularity ($\delta \approx 0.2$) configuration with q_{95}=3.3, and I_p=1-2.6MA. It should be noted, however, that the hydrogen and tritium data is taken from experiments performed in the JET MkIIa divertor. As can be seen from the figure, energy confinement in helium-4 plasmas lies below that of hydrogen plasmas. Thus, for the low activation phase of a next step machine, hydrogen plasmas would be expected to have better performance.

5.2 TYPE III ELMS

Figure 11 shows $H_{IPB98(y,2)}$ for the full JET database of steady helium-4 ELMy H-modes. The fall in confinement, as one moves from Type I (mean $H_{IPB98(y,2)}$=0.77±0.04), to compound Type I-III (mean $H_{IPB98(y,2)}$=0.54±0.03) and Type III (mean $H_{IPB98(y,2)}$=0.46±0.05) ELMy H-modes, is clear. Correcting for the isotope charge scaling, using equation 8, helium-4 Type III ELMy H-modes have an energy confinement time 35% of that seen for helium-4 Type I ELMy H-modes. This is a somewhat larger fall than is usually observed in deuterium H-modes at JET [31].

5.3 NON-DIMENSIONAL PARAMETERS

The difference in confinement between hydrogenic and helium-4 plasmas can also be expressed in terms of non-dimensional parameters. For a given configuration and q-profile, single ion species equipartioned plasmas dominated by high-β transport have been shown theoretically [38, 39, 40] to have a normalised confinement time, $\omega_{ci}\tau_E$, where ω_{ci} is the ion Larmor frequency, which is a function of the non-dimensional plasma parameters ρ_i *, β and ν_{ei} * (see Connor and Taylor [40]

for definitions). If the effects of isotope on the system are included, it is found that no new invariant transforms appear. This may be thought of as being due to the independent Z and M scaling in the ion-ion, electron-electron and ion-electron collisionality. Thus, the energy confinement may be expressed as

$$\omega_{ci}\,\tau_E = F(\rho_i^{*}, \beta, \nu_{ei}^{*}, Z, M; \varepsilon, q, \kappa, \delta, T_i/T_e ...) \quad (9)$$

where, although the ion Larmor frequency, Larmor radius and ion-electron collision time, have been chosen, taking their electron equivalents would merely change the functional dependence on Z and M. This means that identity experiments between different isotopes cannot be performed even with matched ρ_i*, β and ν_{ei}*. However, the functional dependence of Eqn. (9) in terms of Z and M, can be determined.

Log-linear fits to a multi-machine database [12] of hydrogenic ELMy H-modes, have shown that the mass dependence may be represented by the scaling

$$\omega_{ci}\,\tau_E = \rho_i^{-2.70}, \beta^{-0.90}, \nu_{ei}^{-0.0}\, M^{0.96}\, q^{-3.0}\, \varepsilon^{0.73}\, \kappa_a^{2.3} G\,(Z; \delta, T_i/T_e ..) \quad (10)$$

where, $\kappa_a = S/\pi a^2$ is the elongation and S is the area of the poloidal cross section. However, it should be noted that JET experiments with hydrogen and deuterium, which matched ρ_i *, β and ν_{ei} * [39], suggested a much weaker isotope mass dependence. Assuming the form of equation 10, and looking for a power law form for the isotope charge dependence, the best fit to the helium-4 Type I ELMy H-modes and their deuterium references gives

$$G\,(Z; \delta, T_i/T_e ..) = Z^{-1.54\pm0.38}\, H(\delta, T_i/T_e ..) \quad (10)$$

6. SUMMARY

A series of single null, diverted helium-4 H-mode plasmas were performed at JET to improve the understanding of H-mode physics and to investigate their suitability for low activation phases in future tokamak designs, such as ITER.

Argon frosting on the Mark IIGB divertor enabled helium-4 to be pumped successfully. NBI, with sources converted to helium-4 and argon frosting of the cryopanels between discharges, provided up to 12MW of auxiliary heating. Deuterium removal from the near surface wall reservoir [5] meant that helium-4 L-H threshold and Type III ELMy H-mode experiments had high purity (84%-95%), although Type I ELMy H-mode purity was lower (65%-86%).

The L-H power threshold in helium-4 has been shown to have a similar dependency on density and field as for deuterium plasmas, but with an absolute value 42%±10% higher than for a set of

deuterium references. This, together with earlier experiments with hydrogenic species [23], is consistent with a $P_{L-H} \propto M^{-1.1} Z^{1.6}$ isotope scaling. Kiveniemi et al [25] and Hidalgo et al [26] have shown this to be consistent with models based on shear flow stabilisation of edge turbulence. The L-H threshold in helium-4 was also shown to fall, by up to 50%, as the X-point is lowered on to the septum. This is consistent with observations in deuterium [27] and suggests that neutral penetration is important in L-H transition physics.

Both the Type I ELMy H-mode regime and a second ELMy H-mode regime, identified here as the Type III ELMy H-mode in helium-4, have been explored which, for the most part, show the same ELM crash characteristics and occupy the same region of loss power space relative to the L-H threshold. The exception is that ELM frequency increases with increasing power for Type III ELMy H-modes in helium-4, the reverse of the deuterium trend. Energy confinement in helium-4 has $H_{IPB98(y,2)}=0.77\pm0.04$ for Type I ELMy H-modes, compared with $H_{IPB98(y,2)}=1.07\pm0.04$ for the deuterium reference discharges. This has been expressed by the addition of an isotope charge dependency to the ELMy H-mode energy confinement scaling, of the form $\tau_e = Z^{-0.75\pm0.08} \tau_{IPB98(y,2)}$. In dimensionless coordinates, τ_e, normalised by ω_{ci}, is proportional to $M^{0.96} Z^{-1.54}$ for fixed ρ_i^*, β and ν_{ei}^*. For Type III ELMy H-modes in helium-4 plasmas $H_{IPB98(y,2)}=0.46\pm0.05$.

Regarding early operation of ITER in helium-4: JET has demonstrated that Type I and Type III ELMy H-modes can be sustained for many confinement times in helium-4. The L-H power threshold in helium-4 (1.42 times that of deuterium) has been shown to be lower than that in hydrogen (2.0 times that of deuterium), the alternative isotope. This would enable an increased range of field and density to be explored. However, the lower energy confinement in helium-4 (0.68 times that of deuterium) compared with hydrogen (0.87 times that of deuterium) would result in lower normalised pressures.

ACKNOWLEDGEMENTS

This work has been conducted under the European Fusion Development Agreement and is partly funded by EURATOM and the United Kingdom Engineering and Physical Sciences Research Council.

REFERENCES

[1]. W. P. West et al, J. Nucl. Materials **266-269** (1999) 732

[2]. Pitts R. A. et al, J. Nucl. Materials **313-316** (2003) 777, and references therein

[3]. A. Huber et al, "*Tomographic reconstruction of 2-D line radiation distribution in the JET MkIIGB divertor in pure He and D discharges*", to appear in the proceedings of the 30th EPS conference on Controlled Fusion and Plasma Physics, St Petersburg, 2003 (2003)

[4]. M.J. Mantsinen, M.-L. Mayoral, E. Righi, et al., "*ICRF heating scenarios in JET with emphasis on ^{4}He plasmas for the non-activated phase of ITER,*" in Radio-Frequency Power in Plasmas

(Proc. 14th Topical Conference on Radio Frequency Power in Plasmas 7-9th May, 2001, Oxnard, Ca, USA), AIP, New York, p. 59-66

[5]. D. L. Hillis et al, J. Nucl. Materials **313-316** (2003) 1061

[6]. M. E. Fenstermacher et al, J. Nucl. Materials **313-316** (2003) 1206

[7]. C. Challis et al, Nuc. Fus. **29** (1989) 563

[8]. M. O'Mullane et al, in: *Advanced diagnostics for magnetic and inertial fusion*, edited by P. E. Stott, A. Wootton, G. Gorini, E. Sindoni, and D. Batani (Plenum Publishers, New York, 2003) 67

[9]. K-D. Zastrow, M. Brix, C. Giroud, A. Meigs, M. G. O'Mullane, M. Proschek, H. P. Summers, Plasma Phys. Cont. Fusion **45** (2003) 1747

[10]. P. D. Morgan and contributors to the EFDA-JET Work Programme, in: *Advanced diagnostics for magnetic and inertial fusion*, edited by P. E. Stott, A. Wootton, G. Gorini, E. Sindoni, and D. Batani (Plenum Publishers, New York, 2003) 403

[11]. W. Suttrop, F. Ryter, J. G. Cordey et al, "*Testing H-mode parameter similarity in JET and ASDEX Upgrade*", to appear in the proceedings of the 29th EPS conference on Controlled Fusion and Plasma Physics, Montreux, 2002 (2002)

[12]. ITER physics expert group, Nuclear Fusion **39**, 2175 (1999)

[13]. F. Ryter and the H-Mode Database Working Group, Nucl. Fusion **36**, 1217 (1996)

[14]. J. A. Snipes and the International H-mode Threshold Database Working Group, Plasma Phys. Cont. Fusion **42** (2000) A299

[15]. F. Ryter and the H-mode Threshold Database Group, Plasma Phys. Cont. Fusion **44** (2002) A415

[16]. M. Mori et al, Plasma Phys. Cont. Fusion **36** (1994) A39

[17]. F. Ryter et al, Plasma Phys. Cont. Fusion **36** (1994) A99

[18]. S. J. Fielding et al, Plasma Phys. Cont. Fusion **38** (1996) 1091

[19]. J. A. Snipes et al, Plasma Phys. Cont. Fusion **38** (1996) 1127

[20]. T. N. Calstrom and R. J. Groebner, Phys. Plasmas **3** (1996) 1867

[21]. E. Righi et al, Plasma Phys. Cont. Fusion **42** (2000) A199

[22]. L. D. Horton et al, , *"Dependence of the H-mode threshold on the JET divertor geometry*", Maastricht, 1999, ECA **23J** (1999) 193

[23]. E. Righi et al, Plasma Phys. Cont. Fusion **40** (1998) 721

[24]. E. Righi, D. Bartlett, J. P. Christiansen et al, Nucl. Fusion **39**, 309 (1999)

[25]. T. P. Kiviniemi et al, "*L-H transition threshold temperature for helium discharges in JET*", to be presented at the 30th EPS conference on Controlled Fusion and Plasma Physics, St. Petersburg, 2003

[26]. C. Hidalgo et al, J. Nucl. Materials **313-316** (2003) 863

[27]. E. Righi, "Transition to H-mode regime in JET with and without pumped divertors", Proceedings 18th IAEA, 4-10 October 2000, paper IAEA-CN-77/EXP5/31

[28]. L. D. Horton, Plasma Phys. Cont. Fusion **42** (2000) A37
[29]. E. J. Doyle et al, Phys. Fluids B (1991) 3
[30]. H. Zohm, Plasma Phys. Cont. Fusion **38** (1996) 105
[31]. R. Sartori et al, "Study of Type III ELMs in JET", Submitted to Plasma Physics and Controlled Fusion
[32]. R. Sartori, D. Borba, R. Budny et al*, "Confinement loss in JET ELMy H-modes*", Maastricht, 1999, ECA **23J** (1999) 197
[33]. P. C. de Vries, A. Pochelon, M. F. Johnson, M. F. F. Nave, D. F. Howell, O. Sauter and contributors to the EFDA-JET work programme, "*Analysis of shaping effects on sawteeth in JET*", proceedings of the 28th EPS conference on Controlled Fusion and Plasma Physics, Madeira, 2001 (2001)
[34]. M. J. Mantsinen et al, Phys. Rev. Lett. **88** (2002) 105002
[35]. M. Greenwald et al, Nuc. Fus. **28** (1988) 2199
[36]. Rapp J. et al, J. Nucl. Materials **313-316** (2003) 524
[37]. G Saibene, L. D. Horton, R. Sartori et al, Nucl. Fusion **39**, 1133 (1999)
[38]. B. B. Kadomstev, Sov. J. Plasma Phys. **1**, 295 (1975)
[39]. J. G. Cordey et al, Plasma Phys. Controlled Fusion **38**, A67 (1996)
[40]. J. W. Connor and J. B. Taylor, Nucl. Fusion **17**, 1047 (1977)

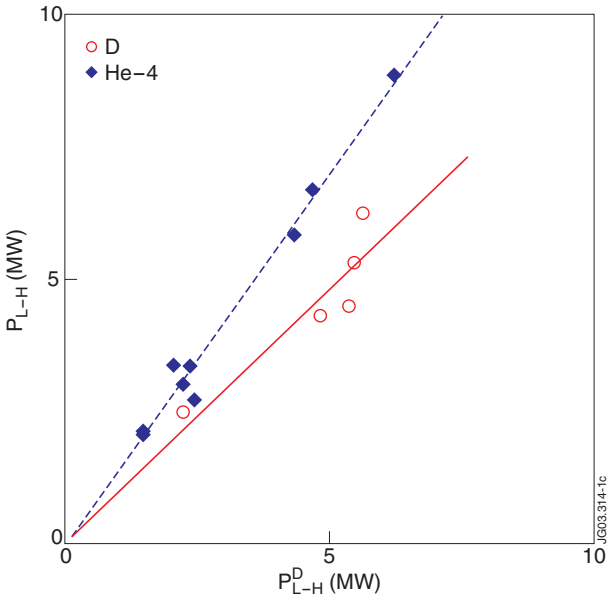

Figure 1: Comparison between the observed L-H power threshold and the scaling law of equation 1 for NBI heated JET Mark IIGB helium-4 (solid blue diamonds) and deuterium reference (open red circles) plasmas. The solid red line represents the multi-machine scaling for deuterium plasmas (1). The broken blue line represents the fit to the helium data (2).

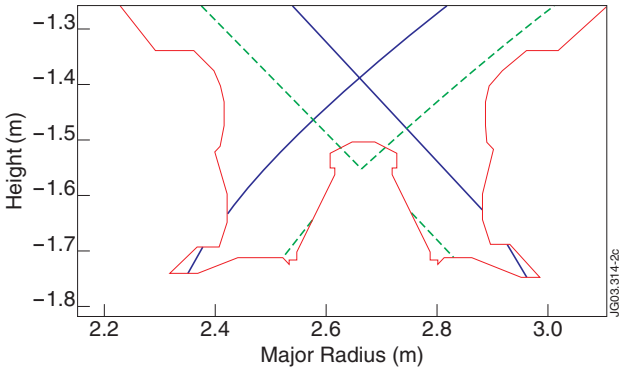

Figure 2: JET Mark IIGB divertor region for the range of configurations used in the L-H power threshold X-pt scan. The height of the X-point varies from 5cm below the septum (broken green line) to 13cm above it (solid blue line).

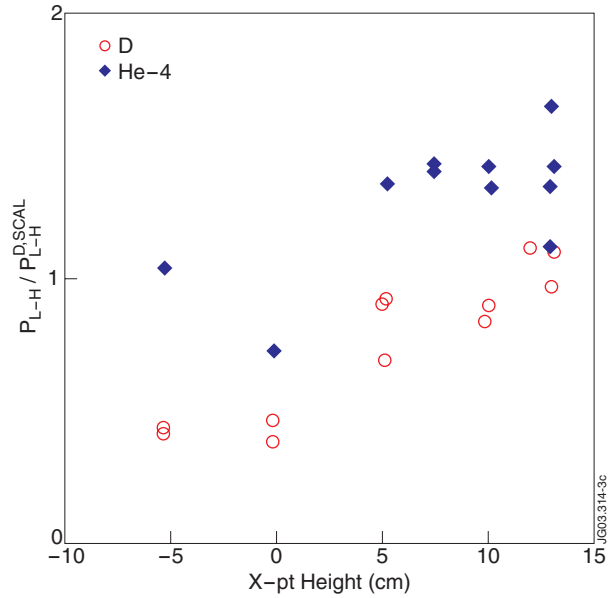

Figure 3: Impact of the X-point height on L-H power threshold for NBI heated helium-4 (solid blue diamonds) and deuterium reference (open red circles) JET Mark IIGB divertor plasmas.

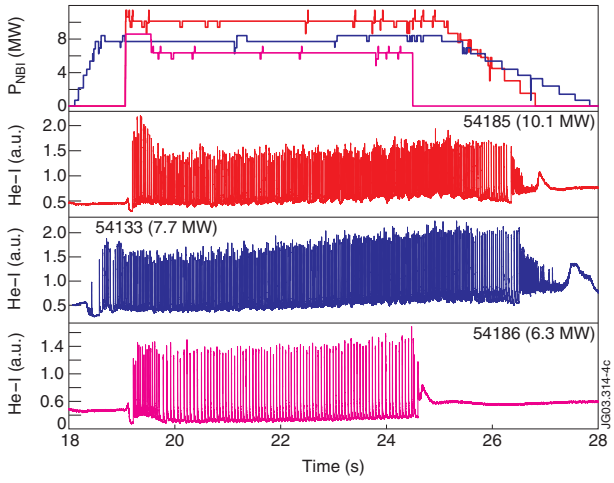

Figure 4: Time traces of three helium-4 ELMy H-mode discharges in a 1MA/1T NBI power scan. The signals shown are the injected NBI power (MW) and the He-I line emission from the outer divertor (arbitrary units).

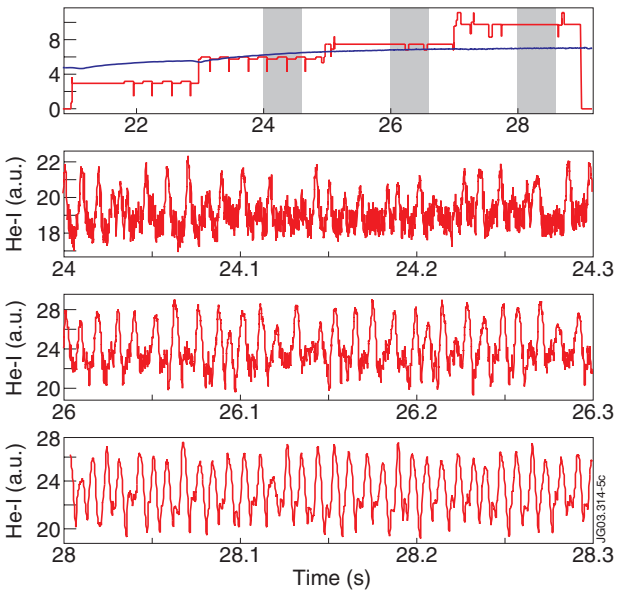

Figure 5: Time trace of JET Pulse no: 54144, a 1.5MA/ 1.5T NBI heated ELMy H-mode helium-4 plasma. The signals shown are the injected NBI power (NBI) and the He-I line emission from the outer divertor (arbitrary units).

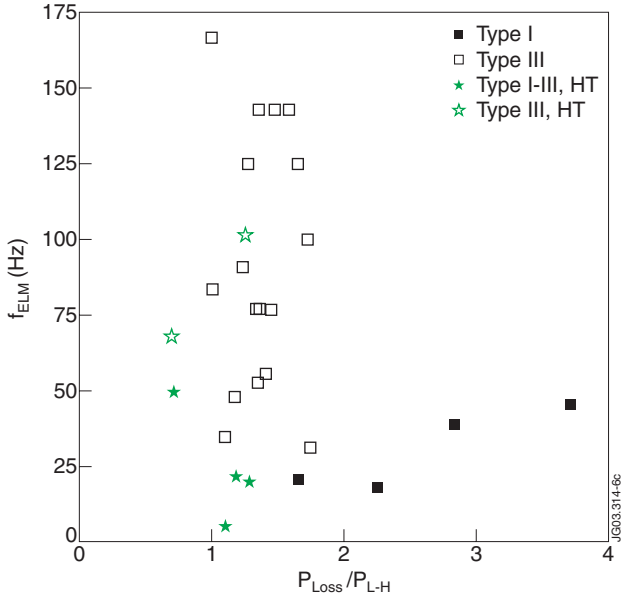

Figure 6: ELM frequency versus loss power through the separatrix, scaled to the helium L-H threshold power (3), for the full database of helium-4 ELMy H-modes. Green stars denote the high triangularity ($\delta \approx 0.4$) configurations and black squares the more standard triangularity ($\delta = 0.2$-0.3) discharges. Open symbols denote Type III ELMy H-modes in helium-4, the solid black squares the Type I ELMy H-modes in low triangularity discharges, and the solid green stars the compound Type I-III ELMy H-modes in high triangularity discharges.

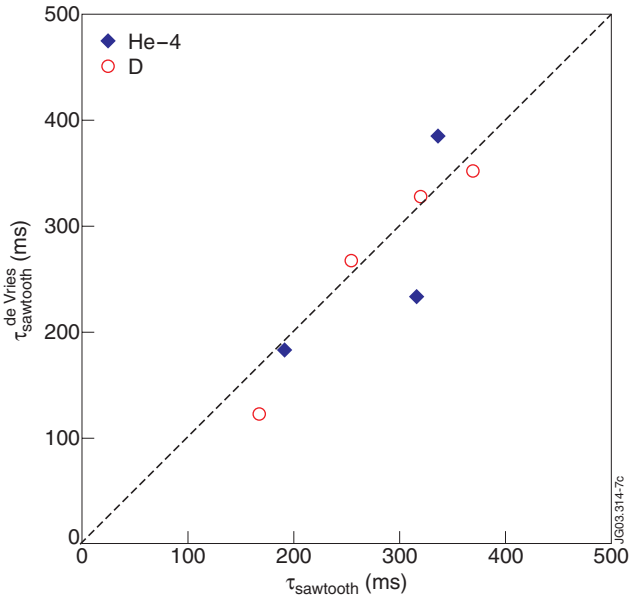

Figure 7: Comparison of the sawtooth period with the scaling law of de Vries et al [33] (6) for helium-4 Type I ELMy H-modes (solid blue diamonds) and their deuterium references (open red circles). The density and temperature are both taken from LIDAR Thomsen scattering, resulting in a time averaged signal, which is multiplied by 10% to approximate the peak measurements.

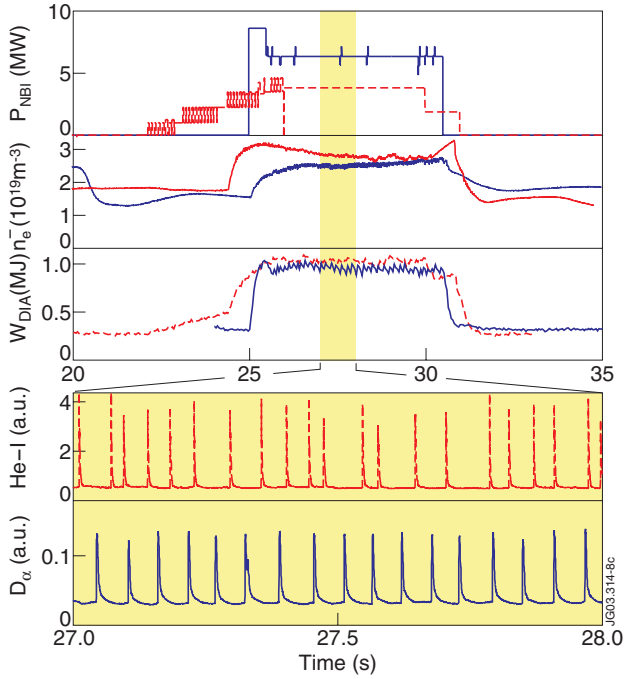

Figure 8: Time trace for a NBI heated Type I ELMy H-mode helium-4 discharge (JET Pulse No: 54186; solid blue line) and its deuterium reference (JET Pulse No: 552949; broken red line), both with 1MA plasma current and 1T toroidal field. The signals shown are the injected NBI power (MW), line averaged electron density (calculated from interferometry), stored energy (MJ), and outer divertor light from the D_α line (for deuterium) and the He-I line (for helium-4).

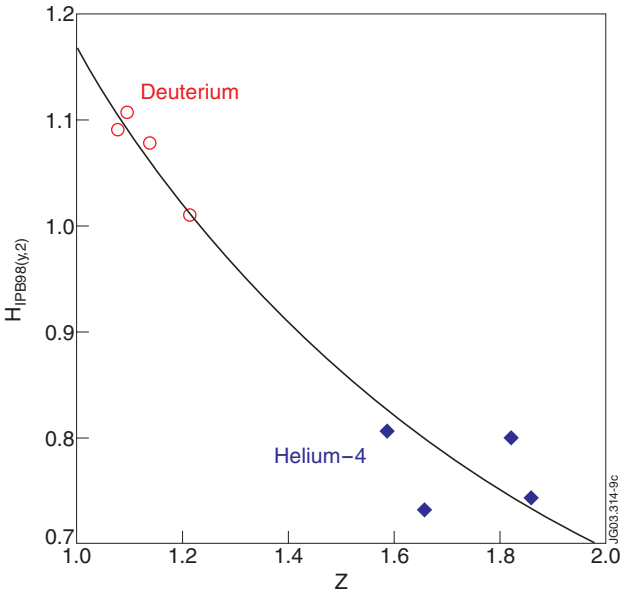

Figure 9: Dependence of the energy confinement time on mean isotope charge for JET Mark IIGB helium-4 (solid blue diamonds) and deuterium reference (open red circles) Type I ELMy H-mode plasmas. The confinement time is normalised to the ELMy H-mode scaling IPB98(y,2) (7). The solid line represents the fit of equation 8.

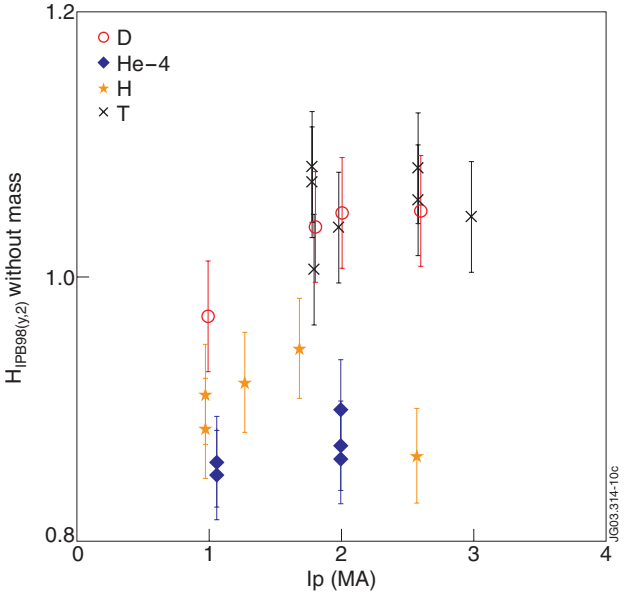

Figure 10: Confinement time, normalised to the ELMy H-mode scaling IPB98(y,2) (7), divided by $(M/2)^{0.19}$ to remove the mass dependence, for JET Mark IIa and Mark IIGB hydrogen (solid yellow stars), deuterium (open red circles), tritium (black crosses) and helium-4 (solid blue diamonds) Type I ELMy H-mode plasmas in the same configuration.

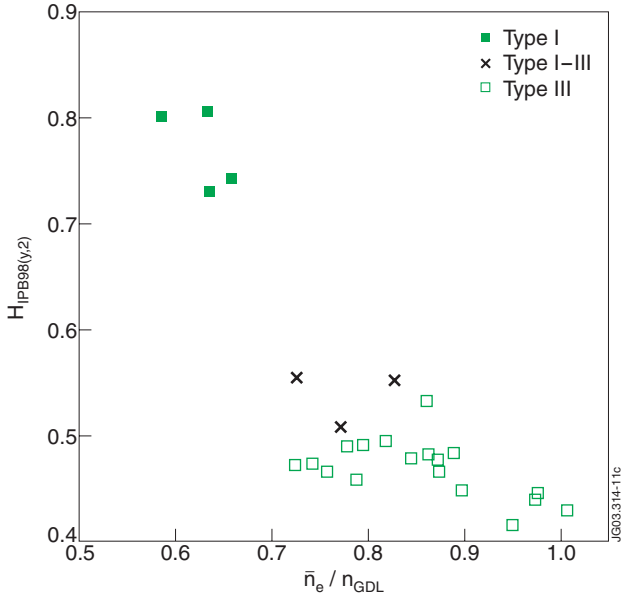

Figure 11: Energy confinement time, normalised to the ELMy H-mode scaling IPB98(y,2) (7), against line averaged density scaled to the Greenwald density limit. Closed green squares denote Type I ELMy H-modes, black crosses denote compound Type I-III ELMy H-modes, and open green circles denote Type III ELMy H-modes in helium-4.